HIGH ANGLE OF ATTACK FLIGHT CHARACTERISTICS OF A WING-IN-PROPELLER-SLIPSTREAM AIRCRAFT

Daisuke Kubo, Koji Muraoka, Noriaki Okada
Japan Aerospace Exploration Agency

Keywords: *Vertical Take-Off and Landing (VTOL), Tail-Sitter Aircraft, Unmanned Aircraft, Wind Tunnel Tests, Flight Tests*

Abstract

A prototype tail-sitter mini unmanned aircraft (SkyEyeV) was developed and tested in a wind tunnel and through automatic flight tests. A tail-sitter is an aircraft that takes off and lands on its tail section with the fuselage pointing upwards. A key feature of the prototype is the leading edge slats, which are incorporated in its design to avoid stall during high angles of attack (AoA) flight. Through wind tunnel tests—aerodynamic force measurements and airflow visualization via the tuft method—it was confirmed that the slats increase the stall AoA not only in the non-powered (without propeller) condition but also in the powered (wing in propeller slipstream) condition. Through automatic high AoA flight tests, the vehicle's flight characteristics were verified and several useful insights were obtained that require further investigation.

1 Introduction

We proposed a new design for a tail-sitter mini unmanned aircraft (UA) in a previous study [1]. Mini UA are small, portable UA that have many applications in various fields, such as, environmental observation, law enforcement, and disaster mitigation [2–4]. However, in spite of the promising potential of mini UA, there are a number of problems associated with their operation. One such problem is their takeoff and landing space requirements. Although mini UA do not require runways and can be operated from a relatively small space, it may still be difficult to find such locations in practice.

The landing performance of mini UA is commonly improved by using parachutes [2] and adopting deep-stall descent [5]. However, these methods also have disadvantages of low accuracy of recovery point and impact shock at touchdown. Another mechanism that improves takeoff and landing performance is vertical takeoff and landing (VTOL). One of the simplest VTOL mechanisms is the tail-sitter. A tail-sitter takes off as well as lands on its tail section with its fuselage pointing upwards. Tail-sitters have the advantage of eliminating the need for variable mechanisms for transition between hovering and cruising, and therefore, this configuration is particularly suitable for mini UA that have strict weight constraints because of their small size.

In a previous research [1], analyses of tail-sitter mini UA's flight characteristics using a mathematical model led to an important finding that leading edge (LE) slats improve descent performance during low-speed, high angle of attack (AoA) transitional flight. In order to experimentally demonstrate the effect of slats, we have developed a prototype of a tail-sitter mini UA called SkyEyeV and verified its basic aerodynamic characteristics by wind tunnel tests [6]. In particular, we observed the airflow over the main wing at high AoA was observed in a wind tunnel using the tuft method and verified the effect of slats. In addition, we conducted high AoA flight tests on the prototype. Here, we present the preliminary results of the tests and clarify some issues.

2 Tail-Sitter Mini Unmanned Aircraft (SkyEyeV)

2.1 Prototype: SkyEyeV

We proposed a new tail-sitter mini UA design in the previous study [1]. In order to demonstrate the design's basic performance, a prototype called SkyEyeV (Fig. 1) was developed using low-cost model airplane manufacturing techniques. This aircraft is powered by twin electric motors, has a wingspan of 1.05 m, and weighs 2.6 kg. The wing is equipped with semi-fixed LE slats, which are set to the retracted or extended positions manually on the ground (Fig. 1).

The aircraft uses propeller slipstream effect to avoid stall during high AoA flight (i.e., the transition between cruise and hover) and for attitude control in low-speed flight. However, this effect is considered to be inefficient in avoiding stall within a certain low airspeed region [1]. This poses a grave problem for tail-sitter mini UA, because a mini UA has relatively low wing loading and flies at relatively low speeds even at flight conditions where the aircraft is kept airborne mainly by the lift force acting on the main wing instead of the thrust force due to the propeller. In order to solve this problem, the proposed design is equipped with the LE slats, whose effect has been simulated in the previous study [1].

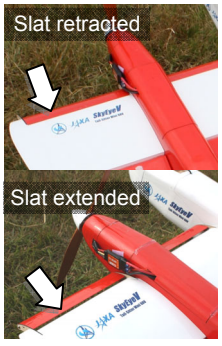

Wingspan:	1.05 m
Length:	0.98 m
Wing area:	0.258 m^2
T/O weight:	2.6 kg
Airfoil:	Clark Y
Leading edge slat:	Semi-fixed, ref. 7 (Fig. 2)
Propeller:	12 in × 6 in (Contra rot., up at tip dir.)
Motor:	Outrunner brushless

Fig. 1 Prototype of tail-sitter mini UA—SkyEyeV

2.2 Operational Scenario

The operational scenario assumed is illustrated in Fig. 2. During takeoff, the vehicle is launched by hand or by support equipment and climbs vertically to a certain altitude. The vehicle then increases its flight speed and switches to forward wing-borne flight; this is called outbound transition. After completing its mission, the vehicle approaches a designated landing point. It reduces the flight speed and switches to the hovering mode; this is called inbound transition. During the final landing phase, the vehicle descends vertically and touches down on its tail landing gear, then drops forward to touch down on its main landing gear, and finally comes to rest on both tail and main landing gears.

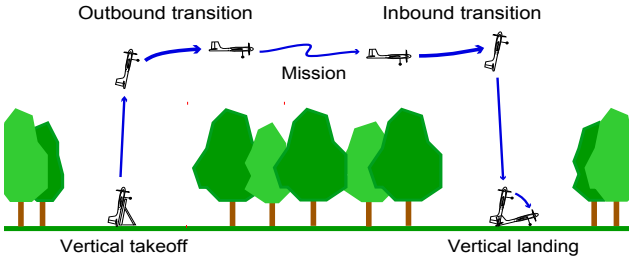

Fig. 2 Operational scenario of tail-sitter mini UA over forest area in VTOL operation

3 Powered Wind Tunnel Tests

3.1 Experimental Settings

Wind tunnel tests were conducted in order to evaluate the vehicle's aerodynamic characteristics, particularly the effect of LE slats. The flight model (prototype) itself was used as the wind tunnel model. The propellers were driven by power supplied from batteries installed in the fuselage, and the rotational

speed of the propeller and the angle of aerodynamic surfaces (ailerons, elevators, and rudders) were controlled using a wireless remote. Therefore, there was no wire between the model and external equipments, which means there was no mechanical interference to the force balance installed between the model and the support sting.

The tests were conducted in JAXA's 2 m × 2 m low-speed wind tunnel, a closed circuit tunnel having a 2 m × 2 m cross-section and a 4 m long test section.

In order to measure aerodynamic characteristics over a wide range of AoA, the support rod had an AoA offset pivot with steps 30° apart: 0°, +30°, and +60°. Since the sting arm traveled from –10° to +30°, the AoA of the vehicle could be set anywhere between –10° and +90° (Figs. 3 and 4). The data presented in this paper were measured at various AoA, 2° apart. Since no wall effect correction method has been established thus far for high AoA maneuvers during powered flight, the data presented in this paper are not corrected for the wall effect.

3.2 Effect of Leading Edge Slats (Without Propeller)

LE slats expand an aircraft's flight envelope by delaying stall. The longitudinal aerodynamic coefficient curves under two different conditions—(1) LE slats retracted (SR) and (2) LE slats extended (SE)—are plotted in Fig. 5. With SR, the vehicle stalls at $\alpha \approx 16°$, whereas with SE, it does not stall at the same angle. In addition, deployment of LE slats delays the increment in C_D due to stall from $\alpha = 14°$ to $\alpha = 30°$, and the change in C_m due to stall becomes more gradual.

The airflow around the main wing was also visualized, and the results are shown in Figs. 6 and 7. The wind speed setting was increased (to

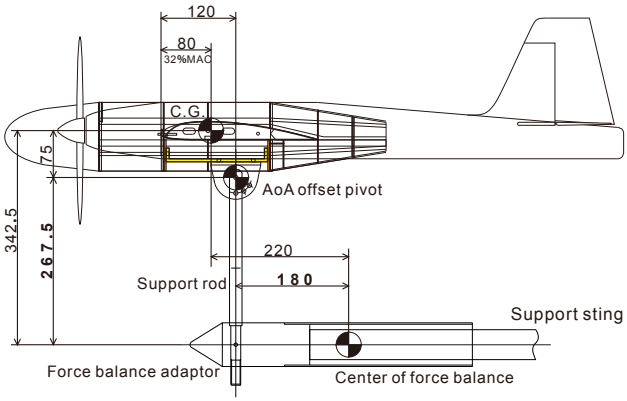

Fig. 3 Wind tunnel model setting

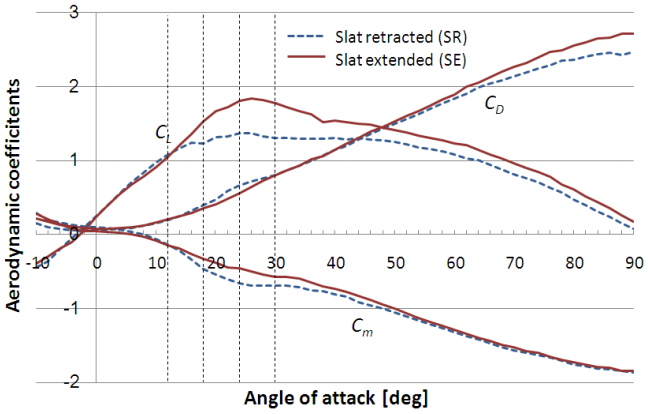

Fig. 5 Non-powered (without propeller) aerodynamic coefficients of SkyEyeV from –10° to +90° ($Re = 1.9 \times 10^5$)

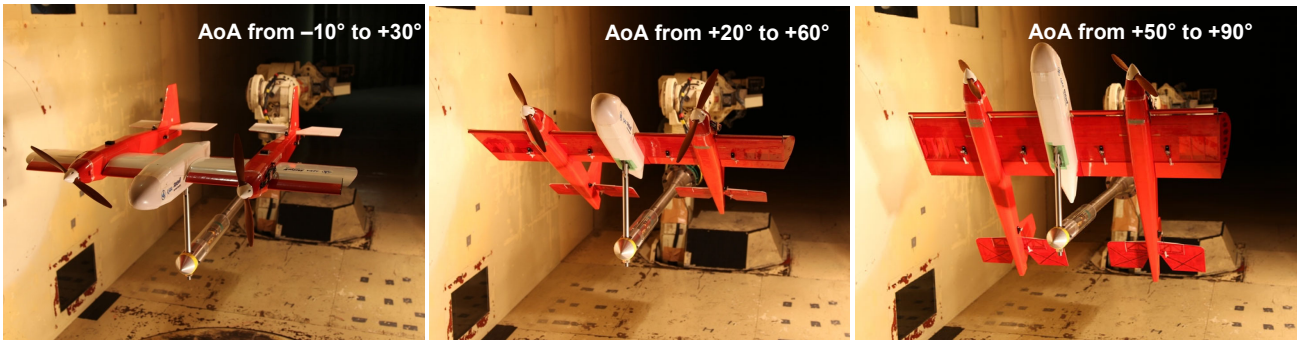

Fig. 4 Wind tunnel model with extended LE slats mounted on support sting with AoA offset $\alpha_{offset} = 0°$ (left), $\alpha_{offset} = +30°$ (center), and $\alpha_{offset} = +60°$ (right)

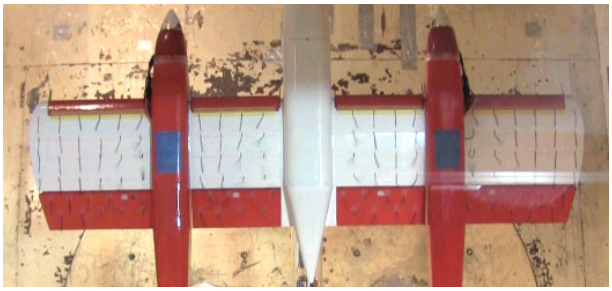

(a) α = 12°: flow separation from trailing edge of inboard wing

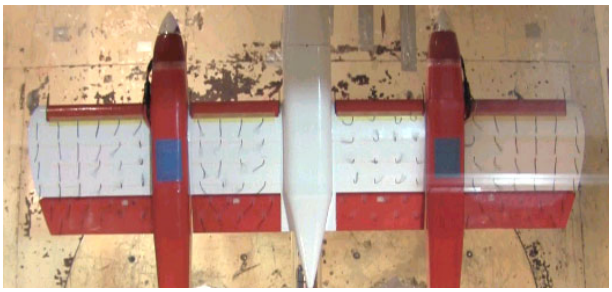

(b) α = 18°: progression of flow separation

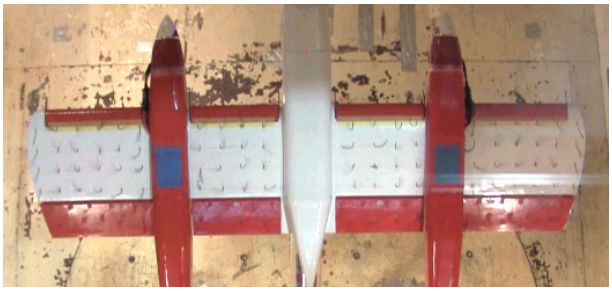

(c) α = 24°: completely separated flow

Fig. 6 Non-powered (without propeller) airflow visualization around main wing of SkyEyeV using tuft method (slats retracted (SR), $Re = 2.9 \times 10^5$)

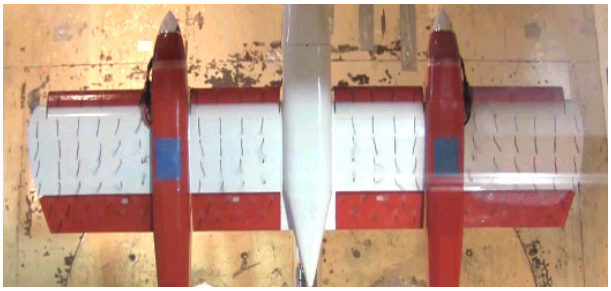

(a) α = 18°: flow separation from trailing edge of inboard wing

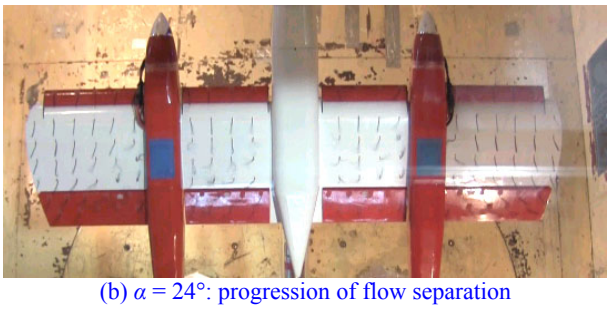

(b) α = 24°: progression of flow separation

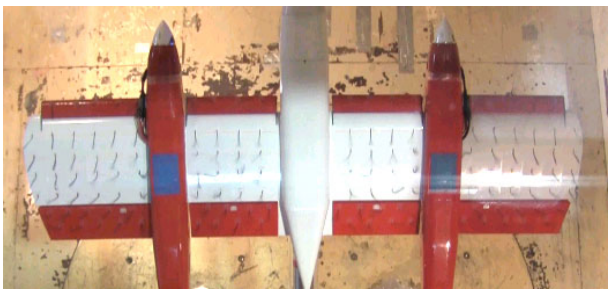

(c) α = 30°: progression of flow separation

Fig. 7 Non-powered (without propeller) airflow visualization around main wing of SkyEyeV using tuft method (slats extended (SE), $Re = 2.9 \times 10^5$)

V = 15 m/s, $Re = 2.9 \times 10^5$) for easy observation. With SR (Fig. 6), flow separation began from the trailing edge of the inboard wing. It gradually continued to separate with the increment in AoA, and the airflow was completely separated at $\alpha \approx 24°$. However, with SE (Fig. 7), the flow separation was delayed and progressed more slowly than in the SR configuration.

3.3 Effect of Propeller Slipstream (in Powered Condition)

For powered tests, apart from the Reynolds number effect, the aerodynamic phenomena of the propeller-wing combination is characterized by the ratio of free stream velocity V m/s to propeller rotation speed ω rad/s. Therefore, we have varied the advance ratio J under different wind tunnel test conditions, where J is defined as

$$J = \frac{2\pi V}{\omega D} \qquad (1)$$

Here, D is the propeller diameter.

The aerodynamic coefficient curves for J = 0.303 are plotted in Fig. 8. The effect of thrust is included in the coefficients C_L, C_D, and C_m.

We will now estimate the trim condition from this data and discuss the effect of LE slats on this trim condition in the case of powered flight. Firstly, we consider the SR case. At $\alpha \approx 25°$, the drag coefficient C_D becomes zero. In steady level flight, this means that the horizontal forces are balanced when the pitch attitude θ = 25° for J = 0.303. Moreover, in order to balance the vertical forces, $L = W$, and the trim airspeed at the power condition $V_{\mathrm{trim},J=0.303}$, should be

$$V_{trim,J=0.303} = \sqrt{\frac{2W}{\rho C_L S}} \qquad (2)$$

where W is the weight of the vehicle and ρ is the air density. Using the experimental data, we obtain $V_{\mathrm{trim},J=0.303}$ = 7.0 m/s. On the other hand, with SE, $V_{\mathrm{trim},J=0.303}$ = 6.7 m/s at θ = 28°.

Conversely, we can identify the stall points from the graph; with SR, this point is to the left of the trimmed condition, while with SE, it is to the right. This means that with SR, the trimmed state at $V_{\mathrm{trim},J=0.303}$ = 7.0 m/s is in the post-stall regime, whereas with SE, the trimmed state at $V_{\mathrm{trim},J=0.303}$ = 6.7 m/s is in the pre-stall regime.

The results of airflow observation are shown in Figs. 9 and 10. The wind speed setting was the same as that used for aerodynamic force measurement (V = 10 m/s, Re = 1.9 × 10^5). With SR (Fig. 9), the flow separation was smaller than that in the non-powered case (Fig. 6) due to the propeller slipstreams. However, the flow separation progressed over the entire wing at α ≈ 24°. With SE (Fig. 10), flow separation was

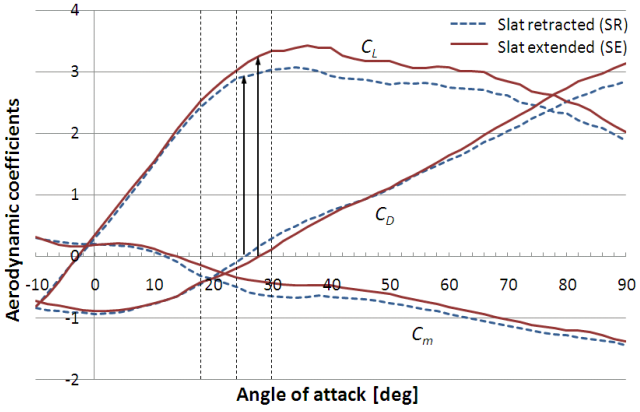

Fig. 8 Powered aerodynamic coefficients of SkyEyeV from –10° to +90° (J = 0.303, Re = 1.9 × 10^5)

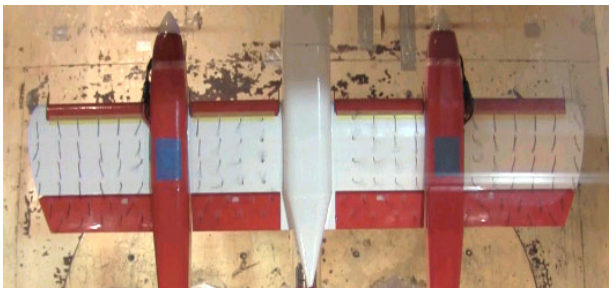

(a) α = 18°: flow separation suppressed by slipstreams

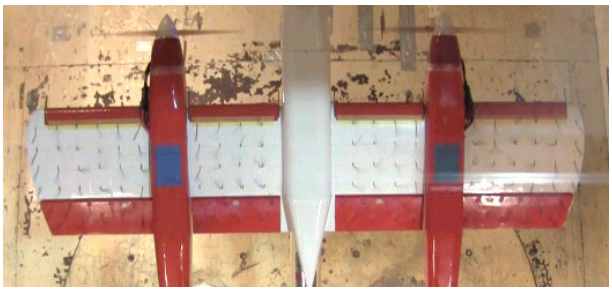

(b) α = 24°: flow separation progressing over the entire wing

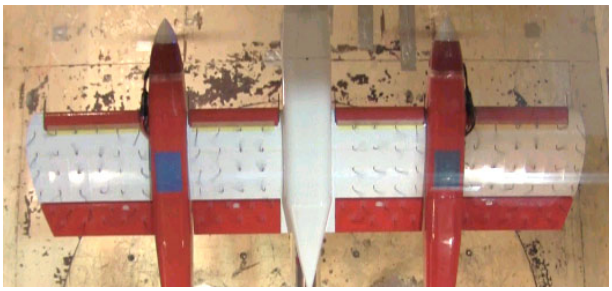

(c) α = 30°: completely separated flow

Fig. 9 Powered (with propeller) airflow visualization around main wing of SkyEyeV using tuft method (slats retracted (SR), Re = 1.9 × 10^5)

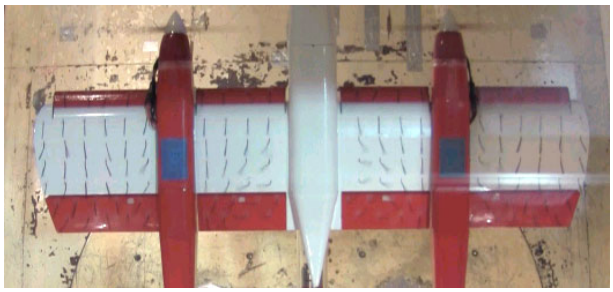

(a) α = 18°: flow separation suppressed by slipstreams

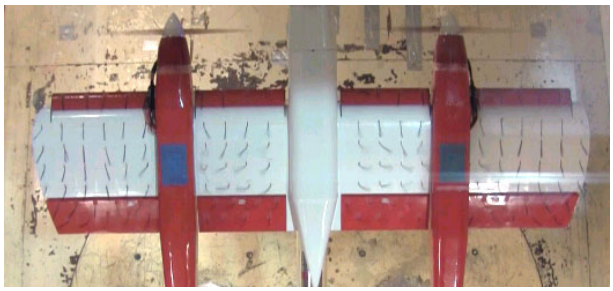

(b) α = 24°: flow separation limited to the inboard wing

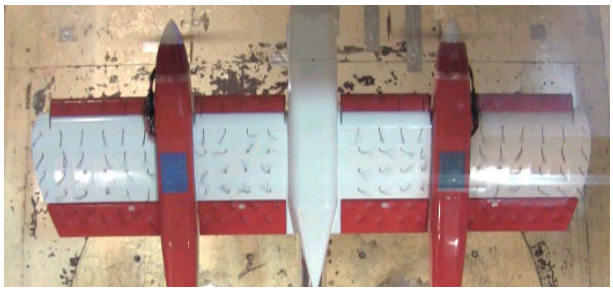

(c) α = 30°: flow separation progressed to the outboard wing

Fig. 10 Powered (with propeller) airflow visualization around main wing of SkyEyeV using tuft method (slats extended (SE), Re = 1.9 × 10^5)

delayed; however, with SE, it was limited to the inboard wing at α = 24° in spite of the separation on the whole wing with SR. Even at α = 30°, the flow separation did not progress over the entire wing.

3.4 Discussions

The results for both aerodynamic force measurements as well as flow visualization show the effectiveness of LE stats in avoiding stall.

In particular, through trim condition analysis in powered flight conditions, it was shown that trimming with SR occurs in the post-stall regime whereas with SE it was in the pre-stall regime. Since the C_L curve, even for the SR case, is continuous around the estimated stall point, longitudinal dynamics may not be largely affected. However, additional aileron deflections may cause serious tip-stall and lateral dynamics may be affected. This issue will be investigated in detail in the future.

4 High Angle of Attack Flight Tests

4.1 Experimental Settings

High AoA flight tests were performed to evaluate the vehicle's flight characteristics during actual flight. An autopilot system, illustrated in Fig. 11, was installed in the vehicle for the flight tests. The system was specially designed for mini UA and is currently under development. It is based on a small commercial GPS/INS unit, in which the attitude estimation is based on quaternion and has no singularity. This feature is appropriate for tail-sitters because of their wide range of attitudes during flight (from cruising to hovering, $\theta \approx 0°$ to 90°).

4.2 Controls

Current results were obtained under the following control conditions:

- ✓ Roll angle: controlled to zero using ailerons (PD control)
- ✓ Yaw angle (flight direction): controlled to the target direction using the rudders (PD control)

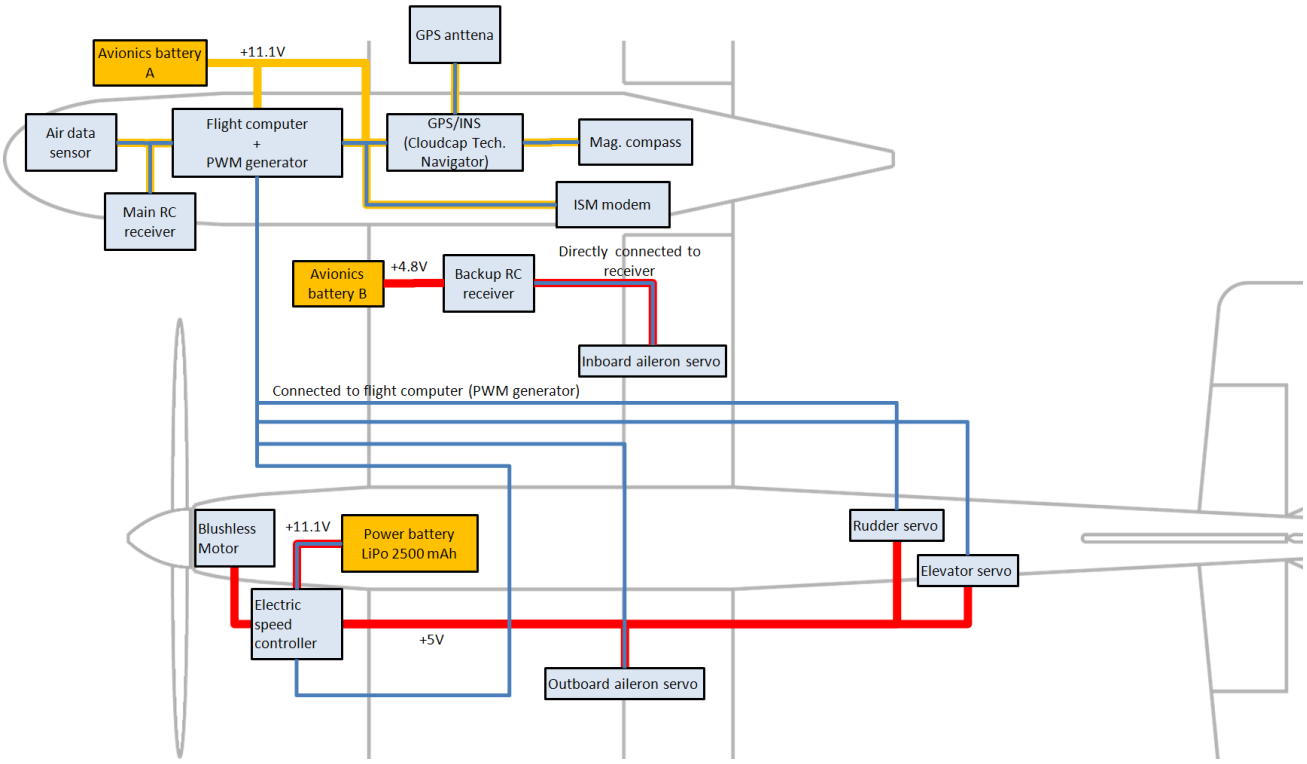

Fig. 11 Schematic illustration of avionics system for SkyEyeV

- ✓ Propeller rotation speeds: controlled to the constant target rotation speed using the throttle (Feedforward and PI control)
- ✓ Pitch angle: controlled to the target angle (from 20° to 50° with 10° steps) using elevators

4.3 Flight

The vehicle took off horizontally via manual control by the remote pilot. After climbing to cruising altitude and turning to the windward direction, which was set as the target direction in yaw control, the pilot switches the control mode from manual to full-automatic. After automatic straight flight of approximately 20 sec, the pilot switches back to the manual mode and circles back the vehicle. This flight pattern was repeated for each target pitch angle θ_{tar} with 10° step.

The weather was calm, and the average wind speed at the flight altitude was estimated to be approximately 2.5 m/s.

Fig. 12 Composite image obtained from a sequence of photographs of high AoA descent flight (wind condition: approx. 2.5 m/s windward, propeller rotation speed: 5500 rpm, photo shoot intervals: not constant (approx. from 0.5 to 0.75 sec))

4.4 Results and Discussions

The flight data histories are plotted in Figs. 13 and 14. Fig. 13 shows the results for SR, and Fig. 14 shows the results for SE. The target propeller rotation speed for both these flights was 6250 rpm. The deflection range of the elevators was from –30° to +50°.

4.4.1 Flights for θ_{tar} = 20°, 30°, and 40°

At target pitch angles θ_{tar} = 20°, 30°, and 40°, the pitch angle responses were stable and the tracking errors were sufficiently small in both SR and SE configurations. Since the rates of climb and flight path angles for these flights were positive, they are not high AoA flights.

4.4.2 Flights for θ_{tar} = 50° (with SR)

For the θ_{tar} = 50° flight, the rate of climb was negative and AoA was large (up to 60°) in the SR case.

The pitch angle responses fluctuated and the tracking error remained. Since the horizontal velocity is not sufficiently small around T = 880 sec, the pitch-down momentum acting on the vehicle was still large for this flight condition. Additionally, higher airspeed at high AoA makes the neutral angle of the elevator larger and its effect becomes poor. Therefore, the pitch angle θ could not increase rapidly. This problem should be addressed considering not only a control strategy, but also a navigation strategy for such high AoA flights.

4.4.3 Flights for θ_{tar} = 50° (with SE)

Although the pitch angle responses also fluctuated, a small tracking error remained in the case of SE. It happened unintentionally that the airspeed was sufficiently small and it made the elevator effective in this flight. The fluctuations can be overcome by improving the controller using a gain scheduling technique.

4.4.4 Effect of LE slat and larger θ_{tar} flights

There are no significant advantages of LE slats and its delayed stall angle in these flight data. It will be clear in flight tests with larger θ_{tar} under various flight conditions.

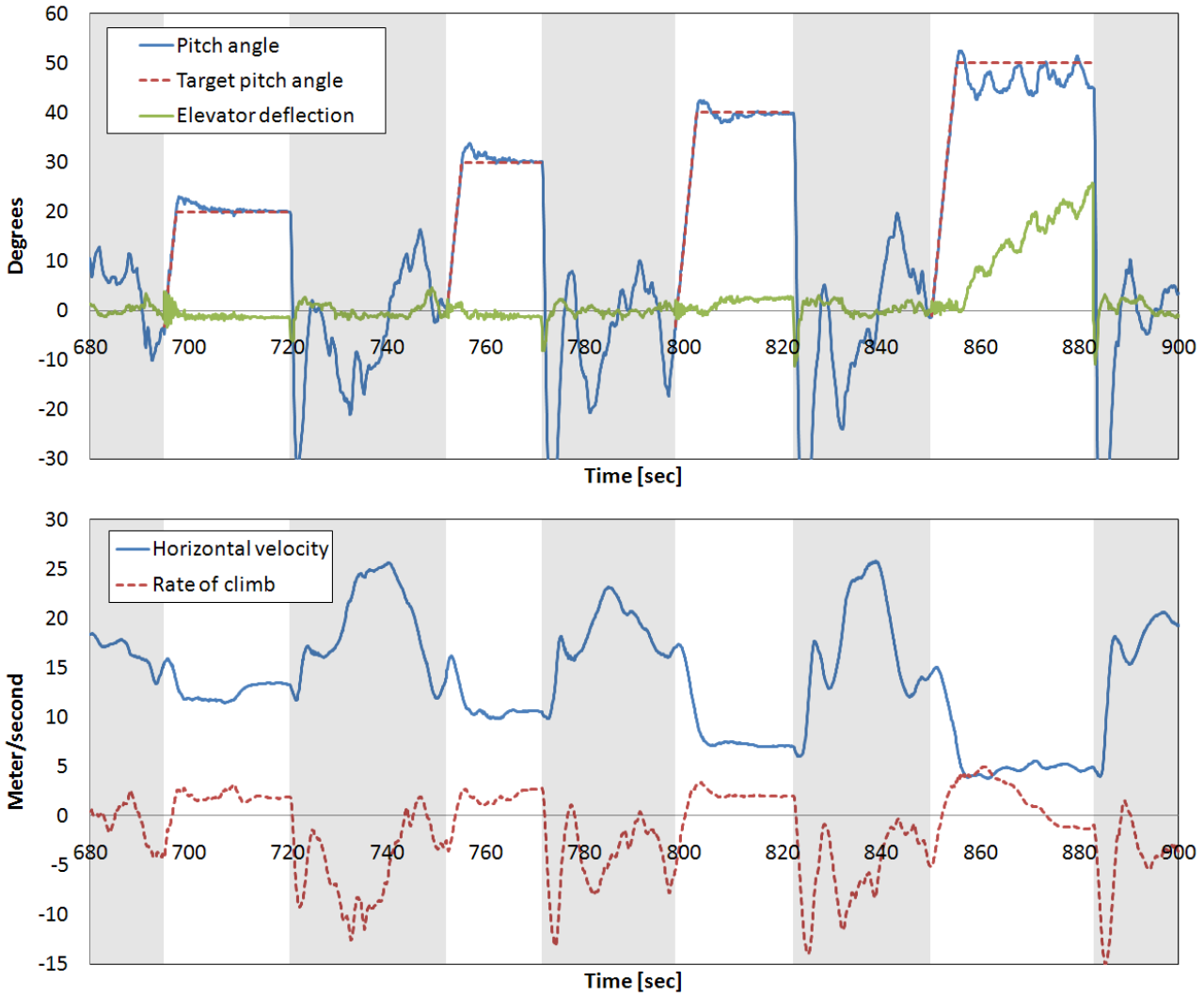

Fig. 13 Flight data histories (LE slats retracted (SR) condition, 6250 rpm)

4.4.5 Elevator deflection for trim

The trim elevator deflections of SE configuration are smaller than those of SR configuration because the deployment of LE slats moved the center of pressure of the vehicle forward and reduced the pitch-down momentum. This is another advantage of using LE slats for high AoA flights.

4.4.6 Control allocation at high AoA

Although flight direction controls were allocated only for rudders in these flight tests, they functioned adequately. For larger θ_{tar} flight, ailerons should also be assigned direction control.

5 Conclusions and Future Work

A tail-sitter mini unmanned aircraft (UA) prototype (SkyEyeV) was developed and wind tunnel tests and automatic high angle of attack (AoA) flight tests were conducted.

The aerodynamic characteristics and effects of leading edge (LE) slats were verified through aerodynamic force measurements and airflow observations using the tuft method. In the non-powered (without propeller) condition, the slats increased the stall AoA from approximately 16° to 26°. Additionally, in the powered condition, there were differences between slats retracted and slats extended configurations. In particular, at an advance ratio of $J = 0.303$, the trimmed condition with LE

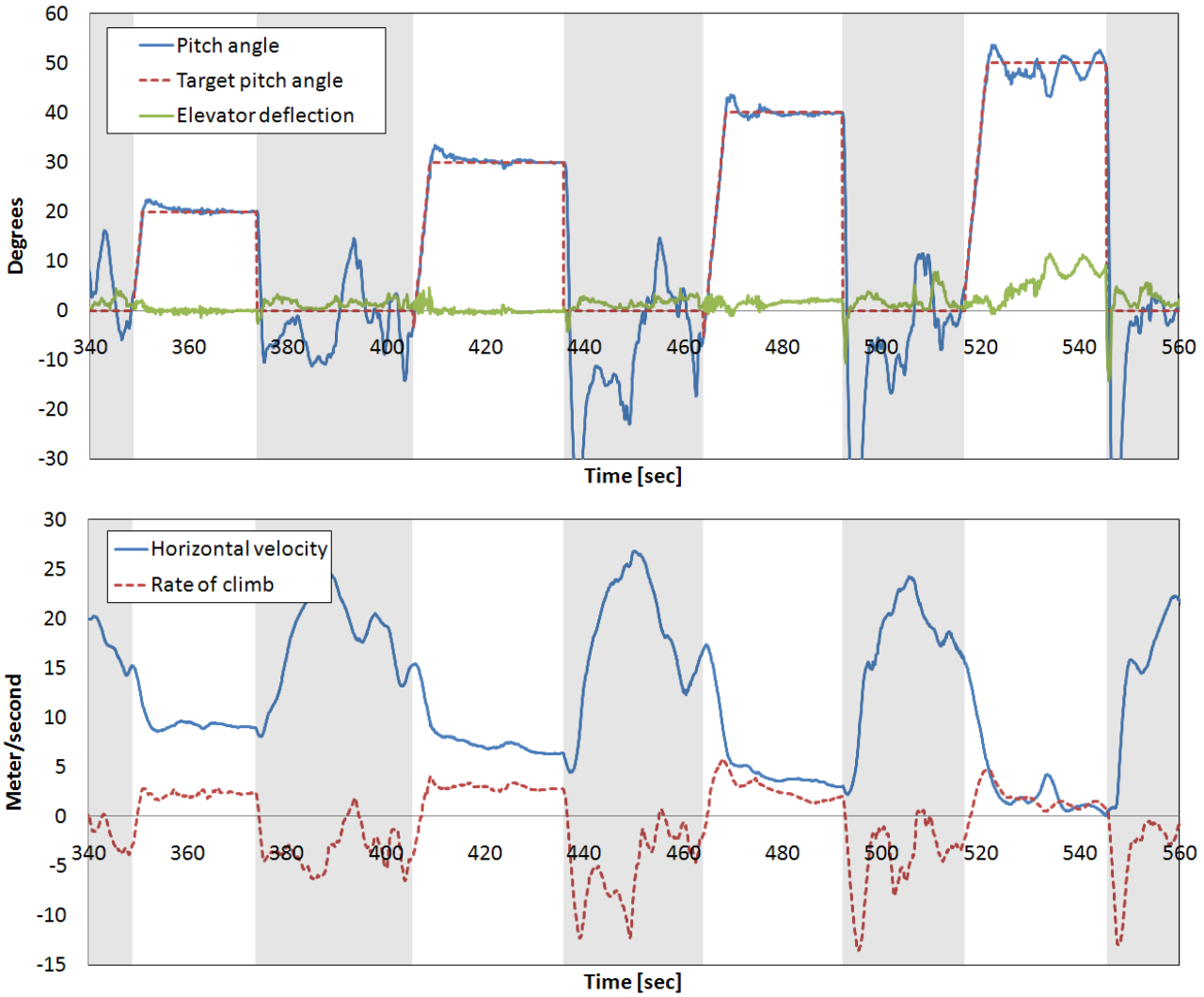

Fig. 14 Flight data histories (LE slats extended (SE) condition, 6250 rpm)

slats retracted lies in the post-stall regime, whereas the trimmed condition with LE slats extended lies in the pre-stall regime. Since flight in post-stall conditions is undesirable because of the unstable aerodynamic characteristics, the effect of LE slats is highly beneficial for the wing-in-propeller-slipstream aircraft.

In automatic flight tests, high AoA flight with pitch angles up to 50° was successfully conducted. However, some technical problems were observed. Airspeed should be reduced before switching to high AoA flight to maintain elevator effectiveness. The pitch angle controller also needs to be improved by using a gain scheduling technique.

We plan to continue this research to investigate and evaluate the effect of LE slats on the flight envelope. We also plan to demonstrate VTOL operations of mini UA and the full mission flights in the near future.

Acknowledgement

This research was conducted in collaboration with the University of Tokyo, Japan. We are grateful to Prof. Shinji Suzuki and members of his laboratory for their contribution to the experiments.

References

[1] Kubo D and Suzuki S. Tail-Sitter Vertical Takeoff and Landing Unmanned Aerial Vehicle: Transitional Flight Analysis, Journal of Aircraft, Vol. 45, No. 1, pp. 292–297, 2008.

[2] Hirokawa R, Kubo D, Suzuki S, Meguro J, and Suzuki T. A Small UAV for Immediate Hazard Map Generation, Proceedings of Infotech@Aerospace 2007, Rohnert Park, California, AIAA Paper 2007-2725, 2007.

[3] Abershitz A, Penn D, Levy A, Shapira A, Shavit Z, and Tsach S. IAI's Micro/Mini UAV Systems-Development Approach, Proceedings of Infotech@Aerospace, Arlington, VA, AIAA Paper 2005-7034, 2005.

[4] Schulz H W, Buschmann M, Kordes T, Kruger L, Winkler S, and Vorsmann P. The Autonomous Micro and Mini UAVs of the CAROLO-Family, Proceedings of Infotech@Aerospace, Arlington, Virginia, AIAA 2005-7092, 2005.

[5] Taniguchi H. Analysis of Deepstall Landing for UAV, Proceedings of ICAS2008, ICAS 2008-5.6.4, 2008.

[6] Kubo D, Muraoka K, Okada N, Naruoka M, Tsuchiya T, and Suzuki S. Flight Tests of a Wing-in-Propeller-Slipstream Mini Unmanned Aerial Vehicle, Proceedings of AIAA Unmanned...Unlimited Conference, Seattle, Washington, AIAA-2009-2070, 2009.

Copyright Statement